to the region of a different function, which smaller-effect substitutions then fine-tune (*24*, *25*); permissive substitutions of small immediate effect, however, precede this process. The intrinsic difficulty of identifying mutations of small effect creates an ascertainment bias in favor of large-effect mutations; the ancestral structures allowed us isolate key combinations of small-effect substitutions from a large set of historical possibilities.

A second contentious issue is whether epistasis makes evolutionary histories contingent on chance events (*26*, *27*). We found several examples of strong epistasis, where substitutions that have very weak effects in isolation are required for the protein to tolerate subsequent mutations that yield a new function. Such permissive mutations create "ridges" connecting functional sequence combinations and narrow the range of selectively accessible pathways, making evolution more predictable (*28*). Whether a ridge is followed, however, may not be a deterministic outcome. If there are few potentially permissive substitutions and these are nearly neutral, then whether they will occur is largely a matter of chance. If the historical "tape of life" could be played again (*29*), the required permissive changes might not happen, and a ridge leading to a new function could become an evolutionary road not taken.

Our results provide insights into the structural mechanisms of epistasis and the historical evolution of new functions. GR's functional specificity evolved by substitutions that destabilized the receptor structure with all hormones but compensated with novel interactions specific to the new ligand. Compensatory mutations have been thought to occur when a second substitution restores a lost molecular interaction (*30*). Our findings support this notion, but in a reversed order: Permissive substitutions stabilized specific structural elements, allowing them to tolerate later destabilizing mutations that conferred a new function (*9*, *10*, *31*). We also observed a more striking mechanism: conformational epistasis, by which one substitution repositions another residue in three-dimensional space and changes the effects of mutations at that site. It is well known that mutations may have nonadditive effects on protein stability (*32*), and fitness (*9*, *33*), but we are aware of few cases (*11*, *34*) specifically documenting new functions or epistasis via conformational remodeling. This may be due to the lack of ancestral structures, which allow evolutionary shifts in the position of specific residues to be determined. Conformational epistasis may be an important theme in structural evolution, playing a role in many cases where new gene functions evolve via novel molecular interactions.

References and Notes

1. G. B. Golding, A. M. Dean, *Mol. Biol. Evol.* **15**, 355 (1998).
2. D. L. Stern, *Evolution Int. J. Org. Evolution* **54**, 1079 (2000).
3. M. F. Perutz, *Mol. Biol. Evol.* **1**, 1 (1983).
4. M. E. Glasner, J. A. Gerlt, P. C. Babbitt, *Curr. Opin. Chem. Biol.* **10**, 492 (2006).
5. L. N. Kinch, N. V. Grishin, *Curr. Opin. Struct. Biol.* **12**, 400 (2002).
6. E. H. Vatzaki *et al.*, *Eur. J. Biochem.* **260**, 176 (1999).
7. O. Khersonsky, C. Roodveldt, D. S. Tawfik, *Curr. Opin. Chem. Biol.* **10**, 498 (2006).
8. F. X. Campbell-Valois, K. Tarassov, S. W. Michnick, *J. Mol. Biol.* **362**, 151 (2006).
9. S. Bershtein, M. Segal, R. Bekerman, N. Tokuriki, D. S. Tawfik, *Nature* **444**, 929 (2006).
10. J. D. Bloom, S. T. Labthavikul, C. R. Otey, F. H. Arnold, *Proc. Natl. Acad. Sci. U.S.A.* **103**, 5869 (2006).
11. J. M. Turner, J. Graziano, G. Spraggon, P. G. Schultz, *Proc. Natl. Acad. Sci. U.S.A.* **103**, 6483 (2006).
12. J. W. Thornton, *Nat. Rev. Genet.* **5**, 366 (2004).
13. J. T. Bridgham, S. M. Carroll, J. W. Thornton, *Science* **312**, 97 (2006).
14. P. J. Bentley, *Comparative Vertebrate Endocrinology* (Cambridge Univ. Press, Cambridge, 1998).
15. A. Sturm *et al.*, *Endocrinology* **146**, 47 (2005).
16. Materials and methods are described in supporting material on *Science* Online.
17. R. L. Wagner *et al.*, *Nature* **378**, 690 (1995).
18. R. K. Bledsoe *et al.*, *J. Biol. Chem.* **280**, 31283 (2005).
19. M. J. Benton, *Vertebrate Palaeontology* (Blackwell Science, Malden, MA, 2005).
20. P. Janvier, *Early Vertebrates* (Clarendon Press, Oxford, 1996).
21. The one-letter abbreviations for the amino acids used in this report are F, Phe; I, Ile; L, Leu; M, Met; N, Asn; P, Pro; Q, Gln; R, Arg; S, Ser; T, Thr; and Y, Tyr. An example of a substitution is Pro for Ser at codon 106 (S106P), and the deletion is in place of Ser at codon 212 (S212Δ).
22. J. M. Smith, *Nature* **225**, 563 (1970).
23. H. A. Orr, *Nat. Rev. Genet.* **6**, 119 (2005).
24. B. Charlesworth, in *Evolutionary Innovations*, M. Nitecki, Ed. (Univ. of Chicago Press, Chicago, 1990), pp. 47–70.
25. H. A. Orr, *Evolution Int. J. Org. Evolution* **56**, 1317 (2002).
26. W. B. Provine, *Origins of Theoretical Population Genetics* (Univ. of Chicago Press, Chicago, 1971).
27. M. C. Whitlock, P. C. Phillips, F. B. G. Moore, S. J. Tonsor, *Annu. Rev. Ecol. Syst.* **26**, 601 (1995).
28. D. M. Weinreich, N. F. Delaney, M. A. Depristo, D. L. Hartl, *Science* **312**, 111 (2006).
29. S. J. Gould, *Wonderful Life: The Burgess Shale and the Nature of History* (Norton, New York, 1989).
30. A. D. Kern, F. A. Kondrashov, *Nat. Genet.* **36**, 1207 (2004).
31. E. S. Haag, M. N. Molla, *Evolution Int. J. Org. Evolution* **59**, 1620 (2005).
32. D. Reichmann *et al.*, *Proc. Natl. Acad. Sci. U.S.A.* **102**, 57 (2005).
33. M. Lunzer, S. P. Miller, R. Felsheim, A. M. Dean, *Science* **310**, 499 (2005).
34. L. Hedstrom, *Biol. Chem.* **377**, 465 (1996).

35. We thank D. Ornoff and J. Bischof for technical assistance and the Thornton, Redinbo, Phillips, and Cresko labs for comments. Supported by NIH-R01-GM081592, NSF-IOB-0546906, and a Sloan fellowship (J.W.T.), NIH-R01-DK622229 (M.R.R.), and NIH-F32-GM074398 (J.T.B.). AncCR crystal structure has Protein Databank identification codes 2Q1H, 2Q1V, and 2Q3Y.

Supporting Online Material

www.sciencemag.org/cgi/content/full/1142819/DC1
Materials and Methods
Figs. S1 to S10
Tables S1 to S5
References

21 March 2007; accepted 6 July 2007
Published online 16 August 2007;
10.1126/science.1142819
Include this information when citing this paper.

A Common Fold Mediates Vertebrate Defense and Bacterial Attack

Carlos J. Rosado,[1,2]* Ashley M. Buckle,[1]* Ruby H. P. Law,[1]* Rebecca E. Butcher,[1,3] Wan-Ting Kan,[1,2] Catherina H. Bird,[1] Kheng Ung,[1] Kylie A. Browne,[4] Katherine Baran,[4] Tanya A. Bashtannyk-Puhalovich,[1] Noel G. Faux,[1] Wilson Wong,[1,2] Corrine J. Porter,[1,2] Robert N. Pike,[1] Andrew M. Ellisdon,[1] Mary C. Pearce,[1] Stephen P. Bottomley,[1] Jonas Emsley,[5] A. Ian Smith,[1,2] Jamie Rossjohn,[1,2] Elizabeth L. Hartland,[6] Ilia Voskoboinik,[4,7] Joseph A. Trapani,[4,8] Phillip I. Bird,[1] Michelle A. Dunstone,[1,6]† James C. Whisstock[1,2]†

Proteins containing membrane attack complex/perforin (MACPF) domains play important roles in vertebrate immunity, embryonic development, and neural-cell migration. In vertebrates, the ninth component of complement and perforin form oligomeric pores that lyse bacteria and kill virus-infected cells, respectively. However, the mechanism of MACPF function is unknown. We determined the crystal structure of a bacterial MACPF protein, Plu-MACPF from *Photorhabdus luminescens*, to 2.0 angstrom resolution. The MACPF domain reveals structural similarity with pore-forming cholesterol-dependent cytolysins (CDCs) from Gram-positive bacteria. This suggests that lytic MACPF proteins may use a CDC-like mechanism to form pores and disrupt cell membranes. Sequence similarity between bacterial and vertebrate MACPF domains suggests that the fold of the CDCs, a family of proteins important for bacterial pathogenesis, is probably used by vertebrates for defense against infection.

The membrane attack complex/perforin (MACPF) domain was originally identified and named as being common to five complement proteins (C6, C7, C8α, C8β, and C9) and perforin (*1*–*3*) (fig. S1). These molecules perform critical functions in innate and

adaptive immunity. Despite limited sequence similarity between their MACPF domains, both perforin and C9 oligomerize and form pores that cause cell lysis (*1*). Complement factors C6 to C9 assemble to form a scaffold [the membrane attack complex (MAC)] that permits C9 polymerization into pores that lyse Gram-negative pathogens. Perforin is delivered by natural killer cells and cytotoxic T lymphocytes and forms oligomeric pores (12 to 18 monomers) in the plasma membrane of either virus-infected or transformed cells (*4*–*7*). Studies on these molecules have shown that the MACPF domain oligomerizes, undergoes conformational change, and is required for lytic activity (*8*, *9*).

Position-Specific Iterated (PSI)–BLAST searches (*10*, *11*) using the sequence of MACPF domains identify >500 proteins with significant expect scores. In addition to proteins involved in invasion and defense (*12*, *13*), family members include nonlytic proteins such as Astrotactin (*14*) (neural migration) and *Drosophila* Torso-like protein (*15*) (embryonic development). Functionally uncharacterized MACPF proteins are also evident in pathogenic bacteria such as *Chlamydia* spp. (*11*) and *Photorhabdus luminescens* (fig. S2). The MACPF family shares 15 to 20% sequence identity within the MACPF domain, and all members include the signature motif Y/W-G-T/S-H-F/Y-X_6-GG, where X is any amino acid (*11*, *16*) (fig. S2).

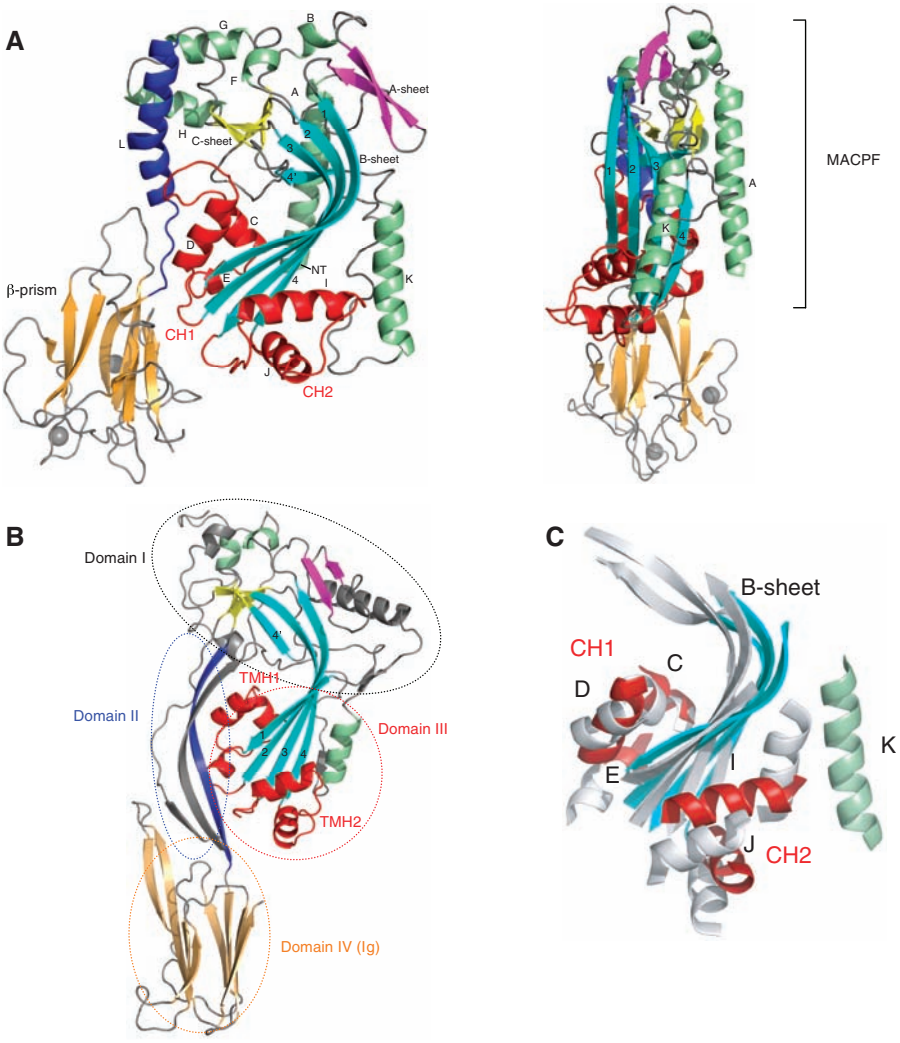

Fig. 1. The structure of Plu-MACPF. (**A**) Secondary-structure elements are labeled (see also fig. S2); CH1 and CH2 are shown in red. Two Cα atoms are shown as gray spheres, and the numbers represent the strand numbering of the B sheet. (**B**) Structure of PFO (*19*). Core elements of secondary structure common to both MACPF and CDCs are colored accordingly. In PFO, the region equivalent to the C sheet in MACPF is continuous with the light blue sheet and is shown in yellow. The first strand of the light blue sheet is shortened and at the top of the sheet, and the region in PFO equivalent to the A sheet (magenta) has collapsed over to form β-sheet hydrogen bonding with the second strand of the light blue sheet. (**C**) Stereo view of the superposition of the core of MACPF and PFO.

We targeted MACPF proteins for structural studies (*17*). Only one of these proteins, Plu-MACPF from *P. luminescens*, expressed solubly and yielded crystals (table S1). Although Plu-MACPF binds to the surface of insect cells (fig. S3), it is nonlytic under a range of conditions (see supporting online material data). However, the structure of its MACPF domain was expected to provide broad insight into the structure and mechanism of function of the MACPF superfamily.

The 2.0 Å crystal structure of Plu-MACPF shows that the 507 residues are divided into an N-terminal MACPF domain and a C-terminal β-prism type I domain (Fig. 1A and fig. S4A). The MACPF domain is a flat box-shaped molecule, featuring a ~50 Å four-stranded antiparallel β sheet (the B sheet) that contains a ~90° twist at strands s4B and s4′B. Two small clusters of α helices [cluster of helices-1 (CH1) and CH2] are packed on each side of the base of the B sheet and form much of the bottom half of the domain (Fig. 1A). The top of the MACPF domain comprises the two-stranded A sheet, the C sheet, and four short α helices (B and F to H). The β-prism domain is underneath CH1 and CH2 and comprises three antiparallel β sheets approximately related by a threefold axis. The β-prism fold is associated with membrane interaction (*18*); however, sequence searching revealed that it is not found in other members of the MACPF superfamily.

Structural characteristics of the MACPF domain, such as its flattened shape and twisted L-shaped central β sheet, bear a striking resemblance to the cholesterol-dependent cytolysin (CDC) family of toxins (*19*). Superpositions and topology diagrams (Fig. 1 and fig. S4) confirmed that the MACPF domain and domains I, II, and III of the archetypal CDC perfringolysin O (PFO) from *Clostridium perfringens* share a common core fold [root mean square (rms) deviation of 3.8 Å per atom over 361 Cα atoms]. The central β sheet, as well as the two clusters of α helices that switch to a membrane-spanning β conformation in PFO [transmembrane β

[1]Department of Biochemistry and Molecular Biology, Monash University, Clayton, VIC 3800, Australia. [2]Australian Research Council (ARC) Centre of Excellence in Structural and Functional Microbial Genomics, Monash University, Clayton, VIC 3800, Australia. [3]Division of Virology, National Institute for Medical Research, The Ridgeway, Mill Hill, London NW7 1AA, UK. [4]Cancer Immunology Program, Peter MacCallum Cancer Centre, St. Andrew's Place, East Melbourne, VIC 3002, Australia. [5]Centre for Biomolecular Sciences, School of Pharmacy, University of Nottingham, Nottingham NG7 2RD, UK. [6]Department of Microbiology, Monash University, Clayton, VIC 3800, Australia. [7]Department of Genetics, University of Melbourne, Parkville, VIC 3010, Australia. [8]Department of Pathology, University of Melbourne, Parkville, VIC 3010, Australia.

*These authors contributed equally to this work.
†To whom correspondence should be addressed. E-mail: michelle.dunstone@med.monash.edu.au (M.A.D.); james.whisstock@med.monash.edu.au (J.C.W.)

hairpin 1 (TMH1) and TMH2, which correspond to CH1 and CH2, respectively, in MACPF], are conserved between the two structures (rms deviation of 0.9 Å per atom over 59 Cα atoms). Only three conserved residues in MACPF (G209, G270, and G271) (fig. S2) are also conserved in the CDC superfamily (equivalent residues in PFO: G274, G324, and G325) (*19*), which explains why PSI-BLAST searches using the MACPF sequences do not identify members of the CDC family with significant expect scores. The N- and C-terminal regions that flank the conserved core, which in PFO correspond largely to the noncontiguous linker domain II, are substantially different. Rather than a single α helix (L helix), the linker in PFO is composed of a twisted β strand supported by an elongated β hairpin derived from the N terminus (Fig. 1B and fig. S4). Despite these differences, the similarity of a complex core fold, together with functional similarities (*20*), suggests that MACPF domains and CDCs are homologous. We therefore propose that lytic MACPF proteins use a CDC-like mechanism of oligomerization and membrane insertion.

CDC-producing Gram-positive pathogens cause mortality in humans. In addition to PFO, well-characterized CDCs include pneumolysin (*Streptococcus pneumoniae*) and streptolysin O (*Streptococcus pyogenes*) (*21*). Like C9 and perforin, CDCs oligomerize, undergo conformational change, and insert into membranes to form doughnut-shaped pores (*22*). The molecular mechanism of pore formation of PFO and pneumolysin is well understood, involving ~30 molecules assembling via the flat faces of the globular head into a pre-pore oligomer that binds the cell membrane via the base of the C-terminal immunoglobulin domain (*19*, *21–24*). A conformational change results in the helical clusters TMH1 and TMH2 of each CDC unravelling to form two elongated amphipathic β hairpins that span the membrane (fig. S5). This converts the pre-pore into a giant β-barrel–lined channel (*19*, *21–24*). Although the amphipathic pattern of amino acids in TMH2 in PFO is imperfect (fig. S6), fluorescence and electron microscopy data reveal that this region is nonetheless able to insert into membranes (*24*). An analysis of the sequence of C9 and perforin also reveals an alternating pattern of hydrophobic and hydrophilic residues in CH1 and CH2, similar to that seen in TMH1 and TMH2 of CDCs and consistent with the ability to form an amphipathic membrane-spanning β hairpin (Fig. 1 and fig. S6). Together with the structural similarity, these data suggest that, rather than using two amphipathic α helices as originally proposed (*25*), lytic MACPF proteins span membranes using amphipathic β strands derived from CH1 and CH2.

Like TMH1 and TMH2 in CDCs, the sequence of CH1 and CH2 represents the most variable region of the superfamily, providing an exception to the general rule that functional elements tend to be highly conserved (*4*, *19*). An analysis of the patterns of conservation in MACPF reveals that the MACPF signature motif Y/W-G-T/S-H-F/Y, originally proposed to form one of two predicted membrane-spanning α helices (*25*), lies at the interface between CH1 and the body of the molecule (Figs. 2 and 3A and table S2). In CDCs, this region undergoes conformational change to allow TMH1 to unfurl (*19*, *22–24*). Another cluster of conserved residues centers on the sharp bend in the B sheet and includes four G residues (G209, G210, G270, and G271) that are >95% conserved in all MACPF proteins (Figs. 2 and 3B). In CDCs, three of these G residues are conserved (G274, G324, and G325 in PFO) and function as a hinge that allows sheet straightening during "hole punching" (*19*, *22–24*). We suggest that these

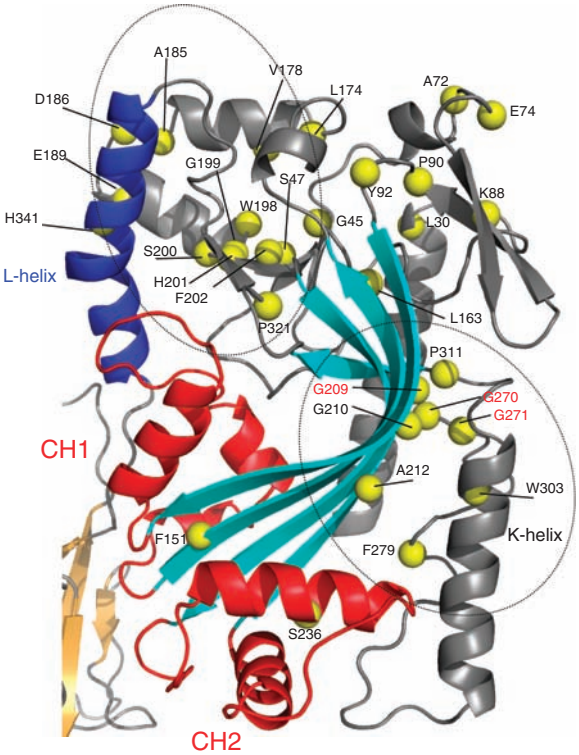

Fig. 2. Sequence conservation in the MACPF domain. Conserved residues in the MACPF family mapped onto the structure of Plu-MACPF (table S2). Three G residues (G209, G270, and G271) are also conserved in CDCs (red text). Two highly conserved clusters are circled, and the numbering is for Plu-MACPF.

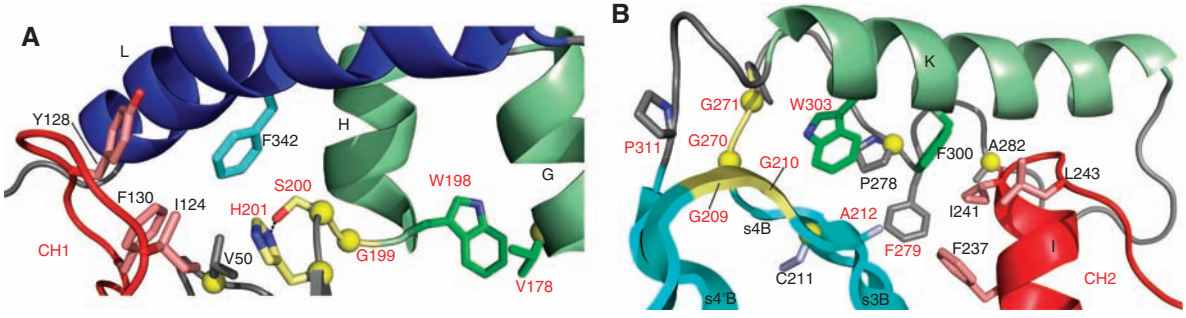

Fig. 3. Atomic interactions made by highly conserved residues. Interactions around (**A**) the conserved signature motif Y/W-G-T/S-H-F/Y and (**B**) the bend in the B sheet. In both panels, red labels indicate conserved residues, and yellow spheres on the Cα position indicate residues that are mutated in FHL. The numbering in both panels is for Plu-MACPF.

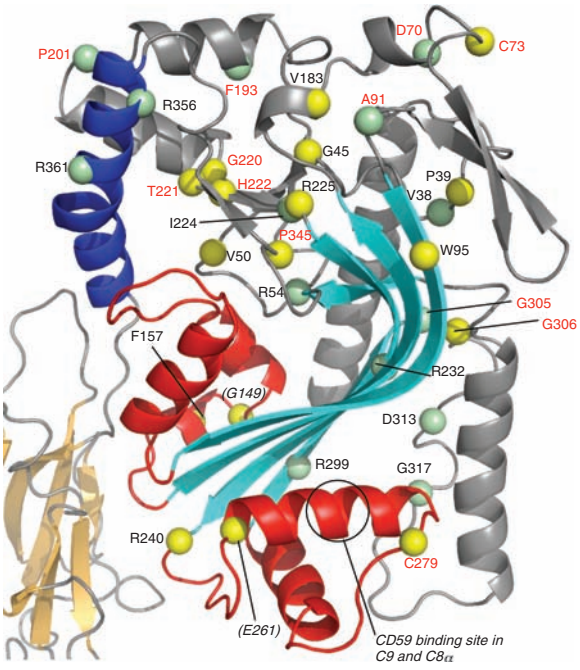

Fig. 4. Position of disease-linked mutations in perforin. The positions of mutations in perforin that cause early onset FHL (yellow) and late onset atypical FHL (pale green) are shown by spheres (table S2). The numbering is for perforin, and red text indicates a mutation of a conserved residue (table S2). The positions of G149 and E261 in perforin are approximate, because these are insertions relative to Plu-MACPF. The position of the CD59 binding site in C9 and C8α is indicated by a black circle (*30*).

residues may permit a similar conformational change in the MACPF domain.

The structure of the MACPF domain gives us a better understanding of mutations in perforin that cause the rare immunological disorder familial hemophagocytic lymphohistiocytosis (FHL) (*4*). In addition to missense mutations of highly conserved residues (Figs. 3 and 4 and table S2), several perforin mutations map to CH1 and CH2 or their surrounding pockets, consistent with a functional role for these regions (Figs. 3 and 4). However, the most intriguing perforin variant identified to date is the A91V (Y92 in Plu-MACPF) polymorphism of perforin which occurs at a frequency of ~3 to 17% and is linked to misfolding, decreased lytic activity, and predisposition to late onset hemophagocytic lymphohistiocytosis (*4*, *26*–*28*). This variant maps to the s2A/s1B loop and its interface with the F helix (Fig. 4). Further, the dysfunctional variant V183G (168 in Plu-MACPF) maps to the F helix and is predicted to pack against A91 (Y92) (Fig. 4). Thus, perturbations of the s2A/s1B–F helix interface may underpin the perforin A91V misfolding phenotype.

Previous studies have shown that C9/MAC activity is controlled by host inhibitors such as CD59 that prevent unwanted cell lysis. Sequences on C9 and C8α that participate in CD59 binding (*29*, *30*) map to CH2 (Fig. 4). Thus, we suggest that CD59 may regulate MAC function by interfering with CH2.

The MACPF domain is commonly found to be associated with other N- and C-terminal modules (fig. S1) that probably control or target MACPF function. For example, the C-terminal C2 domain of perforin mediates initial interactions with membranes (*4*), an analogous role to that of domain IV of the CDCs (*19*).

Although Plu-MACPF appears to be nonlytic under the conditions tested, we cannot exclude the possibility that it requires a cofactor or specific receptor for function. On the other hand, certain MACPF proteins (e.g., C6, C7, C8β, and Astrotactin) do not lyse cells and instead perform other roles. We speculate that certain utilities of the MACPF fold, such as conformational flexibility and membrane insertion, may have been exploited for nonlytic purposes. Indeed, parallels can be drawn with the eukaryote B cell lymphoma 2 family of proteins that share a similar fold to bacterial colicin-like toxins but insert into membranes rather than lyse cells (*31*).

This work implies that lytic members of the MACPF superfamily use a CDC-like mechanism for membrane penetration and pore formation. Our findings suggest that the fold of the CDCs, a family of proteins that causes tissue destruction in human diseases, is used by vertebrates for defense against bacterial and viral infection.

References and Notes

1. J. Tschopp, D. Masson, K. K. Stanley, *Nature* **322**, 831 (1986).
2. Y. Shinkai, K. Takio, K. Okumura, *Nature* **334**, 525 (1988).
3. M. G. Lichtenheld *et al.*, *Nature* **335**, 448 (1988).
4. I. Voskoboinik, M. J. Smyth, J. A. Trapani, *Nat. Rev. Immunol.* **6**, 940 (2006).
5. J. A. Trapani, *Int. Rev. Cytol.* **182**, 111 (1998).
6. D. Keefe *et al.*, *Immunity* **23**, 249 (2005).
7. G. Chen, L. Shi, D. W. Litchfield, A. H. Greenberg, *J. Exp. Med.* **181**, 2295 (1995).
8. R. G. DiScipio, C. Berlin, *Mol. Immunol.* **36**, 575 (1999).
9. M. E. Pipkin, J. Lieberman, *Curr. Opin. Immunol.* **19**, 301 (2007).
10. S. F. Altschul *et al.*, *Nucleic Acids Res.* **25**, 3389 (1997).
11. C. P. Ponting, *Curr. Biol.* **9**, R911 (1999).
12. E. S. Haag, B. J. Sly, M. E. Andrews, R. A. Raff, *Dev. Biol.* **211**, 77 (1999).
13. K. Kadota, T. Ishino, T. Matsuyama, Y. Chinzei, M. Yuda, *Proc. Natl. Acad. Sci. U.S.A.* **101**, 16310 (2004).
14. C. Zheng, N. Heintz, M. E. Hatten, *Science* **272**, 417 (1996).
15. J. R. Martin, A. Raibaud, R. Ollo, *Nature* **367**, 741 (1994).
16. Single-letter abbreviations for the amino acid residues are as follows: A, Ala; C, Cys; D, Asp; E, Glu; F, Phe; G, Gly; H, His; I, Ile; K, Lys; L, Leu; M, Met; N, Asn; P, Pro; Q, Gln; R, Arg; S, Ser; T, Thr; V, Val; W, Trp; and Y, Tyr.
17. Materials and methods are available as supporting material on *Science* Online.
18. J. D. Li, J. Carroll, D. J. Ellar, *Nature* **353**, 815 (1991).
19. J. Rossjohn, S. C. Feil, W. J. McKinstry, R. K. Tweten, M. W. Parker, *Cell* **89**, 685 (1997).
20. A. G. Murzin, *Curr. Opin. Struct. Biol.* **8**, 380 (1998).
21. S. J. Tilley, H. R. Saibil, *Curr. Opin. Struct. Biol.* **16**, 230 (2006).
22. R. J. Gilbert *et al.*, *Cell* **97**, 647 (1999).
23. S. J. Tilley, E. V. Orlova, R. J. Gilbert, P. W. Andrew, H. R. Saibil, *Cell* **121**, 247 (2005).
24. O. Shatursky *et al.*, *Cell* **99**, 293 (1999).
25. M. C. Peitsch *et al.*, *Mol. Immunol.* **27**, 589 (1990).
26. I. Voskoboinik, M. C. Thia, J. A. Trapani, *Blood* **105**, 4700 (2005).
27. C. Trambas *et al.*, *Blood* **106**, 932 (2005).
28. I. Voskoboinik *et al.*, *Blood* **110**, 1184 (2007).
29. D. H. Lockert *et al.*, *J. Biol. Chem.* **270**, 19723 (1995).
30. Y. Huang, F. Qiao, R. Abagyan, S. Hazard, S. Tomlinson, *J. Biol. Chem.* **281**, 27398 (2006).
31. S. W. Muchmore *et al.*, *Nature* **381**, 335 (1996).

32. J.C.W. is a National Health and Medical Research Council (NHMRC) principal research fellow and a Monash University Senior Logan fellow, M.A.D. is an NHMRC Peter Doherty training fellow, A.M.B. and S.P.B. are NHMRC senior research fellows, A.I.S. is an NHMRC principal research fellow, J.R. is an Australian Research Council Federation fellow, I.V. is an NHMRC R. Douglas Wright fellow, and J.A.T. is an NHMRC senior principal research fellow. We thank the NHRMC (program grant numbers 284233 and 454569), the ARC, the Victorian Partnership for Advanced Computing and the Australian Synchrotron Research Program for support, and the staff of the Industrial Macromolecular Crystallography Association–Collaborative Access Team beamline 17ID at the Advanced Photon Source (U.S.A.) for data collection facilities and for technical support. Coordinates and structure factors have been deposited in the Protein Data Bank with accession number 2QP2. Raw diffraction data are available at http://arrow.monash.edu.au/hdl/1959.1/5863 [the Web site for the Monash University institutional repository, using the ARROW (Australian Research Repositories Online to the World) software solution].

Supporting Online Material

www.sciencemag.org/cgi/content/full/1144706/DC1
Materials and Methods
Figs. S1 to S6
Tables S1 and S2
References

7 May 2007; accepted 31 July 2007
Published online 23 August 2007;
10.1126/science.1144706
Include this information when citing this paper.